Liquid Crystals
Publication details, including instructions for authors and subscription information:
http://www.informaworld.com/smpp/title~content=t713926090

Main chain, thermotropic, liquid crystalline, hydrogen-bonded polymers of 4,4'-bipyridyl with 4,4'-dicarboxy-α,ω-diphenoxyalkanes

Pradip K. Bhowmik[a]; Xiaobin Wang[b]; Haesook Han[a]
[a] Department of Chemistry, University of Nevada Las Vegas, Las Vegas, Nevada 89154, USA [b] ITW Plexus, Danvers, Massachusetts 01923, USA

To cite this Article Bhowmik, Pradip K. , Wang, Xiaobin and Han, Haesook(2007) 'Main chain, thermotropic, liquid crystalline, hydrogen-bonded polymers of 4,4'-bipyridyl with 4,4'-dicarboxy-α,ω-diphenoxyalkanes', Liquid Crystals, 34: 7, 841 — 854

To link to this Article: DOI: 10.1080/02678290701379616

URL: http://dx.doi.org/10.1080/02678290701379616

Liquid Crystals, Vol. 34, No. 7, July 2007, 841–854

Main chain, thermotropic, liquid crystalline, hydrogen-bonded polymers of 4,4′-bipyridyl with 4,4′-dicarboxy-*α*,*ω*-diphenoxyalkanes

PRADIP K. BHOWMIK*†, XIAOBIN WANG‡ and HAESOOK HAN†

†Department of Chemistry, University of Nevada Las Vegas, 4505 Maryland Parkway, Box 454003, Las Vegas, Nevada 89154, USA

‡ITW Plexus, 30 Endicott Street, Danvers, Massachusetts 01923, USA

(*Received 24 November 2006; accepted 15 March 2007*)

A series of main chain, thermotropic, liquid crystalline (LC) hydrogen-bonded polymers based on 4,4′-bipyridyl as a hydrogen bond acceptor and 4,4′-dicarboxy-α,ω-diphenoxyalkanes as hydrogen bond donors were prepared by a slow evaporation technique from a pyridine solution and characterized for their thermotropic LC properties using a variety of experimental techniques. The homopolymer of 4,4′-bipyridyl with 4,4′-dicarboxy-1,9-diphenoxynonane exhibited relatively low T_m at 205°C and low T_i at 230°C, giving an LC phase range of 25°C. The other two homopolymers with 4,4′-dicarboxy-1,6-diphenoxyhexane and 4,4′-dicarboxy-1,9-diphenoxydecane exhibited relative low T_m values, above which each of them formed high-order smectic phases. With further heating at higher temperature they transformed into low-order smectic phases that persisted up to their decomposition temperatures. Several copolymers also had relatively low T_m values as well as low T_i values and, therefore, had a broad LC phase range (22–77°C). All of the polymers including copolymers exhibited high-order and low-order smectic phases, since they developed usually mosaic and schlieren (or bâtonnets) textures. Generally, copolymerization increased the temperature range of the LC phases for these polymers. The thermal transitions of all of the polymers were well below their decomposition temperatures, which were in the ranges of 254–329°C.

1. Introduction

The hydrogen bond is a most important interaction and plays a multitude of roles in supramolecular chemistry, from molecular recognition and molecular self-assembly in biological macromolecules, to an increase in polymer miscibility in polymer blends [1–17]. It can also induce liquid crystallinity either in low molar mass organic compounds, or in macromolecules prepared from two suitably designed components that are commonly called H-bond donors and H-bond acceptors [18–30]. Lehn and coworkers [31–35] introduced the concept of using well-defined H-bond secondary interactions in the synthesis and characterization of liquid-crystalline polymers (LCPs); the liquid crystalline properties derive directly from the individual components through triple hydrogen bonding instead of commonly used covalent bonding [36–40]. It is accomplished by mixing long chain derivatives of chiral tartaric acid bifunctionalized by the complementary groups 2,6-diaminopyridine (P) and uracil (U). These two functional groups spontaneously associate via triple H-bonds. The resulting supramolecular polymer appears as a highly birefringent gel that forms fibres on spreading. Whereas the pure components exhibit a complex polymorphism, the mixture displays an LC phase from below room temperature to a temperature higher than 200°C.

The specific chirality of tartaric acid is observed to influence profoundly the superstructure formed. Derivatives of laevo-tartaric acid form columns consisting of three polymeric strands in a triple helix superstructure, whereas those based on meso-tartaric acid form columns built of three strands in zigzag conformation. A mixture based on laevo- and dextro-tartaric acid produces yet another columnar arrangement. The effect of replacing the flexible tartaric acid segment by a rigid 9,10-dialkoxyanthracene core in this supramolecular polymer is also reported. The U and P groups are, in this case, are connected to the anthracene-based core via an imide group, restricting rotation about the C–N bond. The consequence of this increased molecular rigidity is the decomposition of this polymer

---

*Corresponding author. Email: pradip.bhowmik@unlv.edu

Liquid Crystals
ISSN 0267-8292 print/ISSN 1366-5855 online
http://www.tandf.co.uk/journals
DOI: 10.1080/02678290701379616

at about 295°C, prior to the melting transition. Thus, it is not a thermotropic LC polymer; however, it is soluble in 1,1,2,2-tetrachloroethane at room temperature, and forms a viscous, birefringent solution that is indicative of a lyotropic LC phase. The optical texture exhibited by such a solution when viewed through a polarizing optical microscope (POM) suggests that the phase is nematic.

Griffin and coworkers [41–47] studied the thermotropic LC properties of chain-extended supramolecular polymers of various structurally different bispyridyls as H-bond acceptors with [(oxydiethoxyethylene)dioxy]-bis(4-benzoic acid) [also known as tetraethyleneglycoxybis(4-benzoic acid)] as an H-bond donor. The bispyridyls used are *trans*-1,2-bis(4-pyridyl)ethylene, 4,4′-(1,10-decanedioxy)diphenolbis(4-pyridinecarboxylate) and hydroquinonebis(4-pyridinecarboxylate). Each of the polymers forms a nematic LC phase, even though none of the components alone shows any LC properties. Additionally, the supramolecular polymers of *trans*-1,2-bis(4-pyridyl)ethylene with a tetraethyleneglycoxybis(4-benzoic acid) derivative exhibits a smectic A (SmA) phase that is only detectable in the cooling cycle of differential scanning calorimetry (DSC) and is also confirmed by POM studies. These results indicate that the formation of an LC phase in each of the polymers is unrelated to the involvement of the oxyethylene group (spacer) of the diacid in any complexation, because a decamethylene group present in the diacid produces qualitatively similar results,

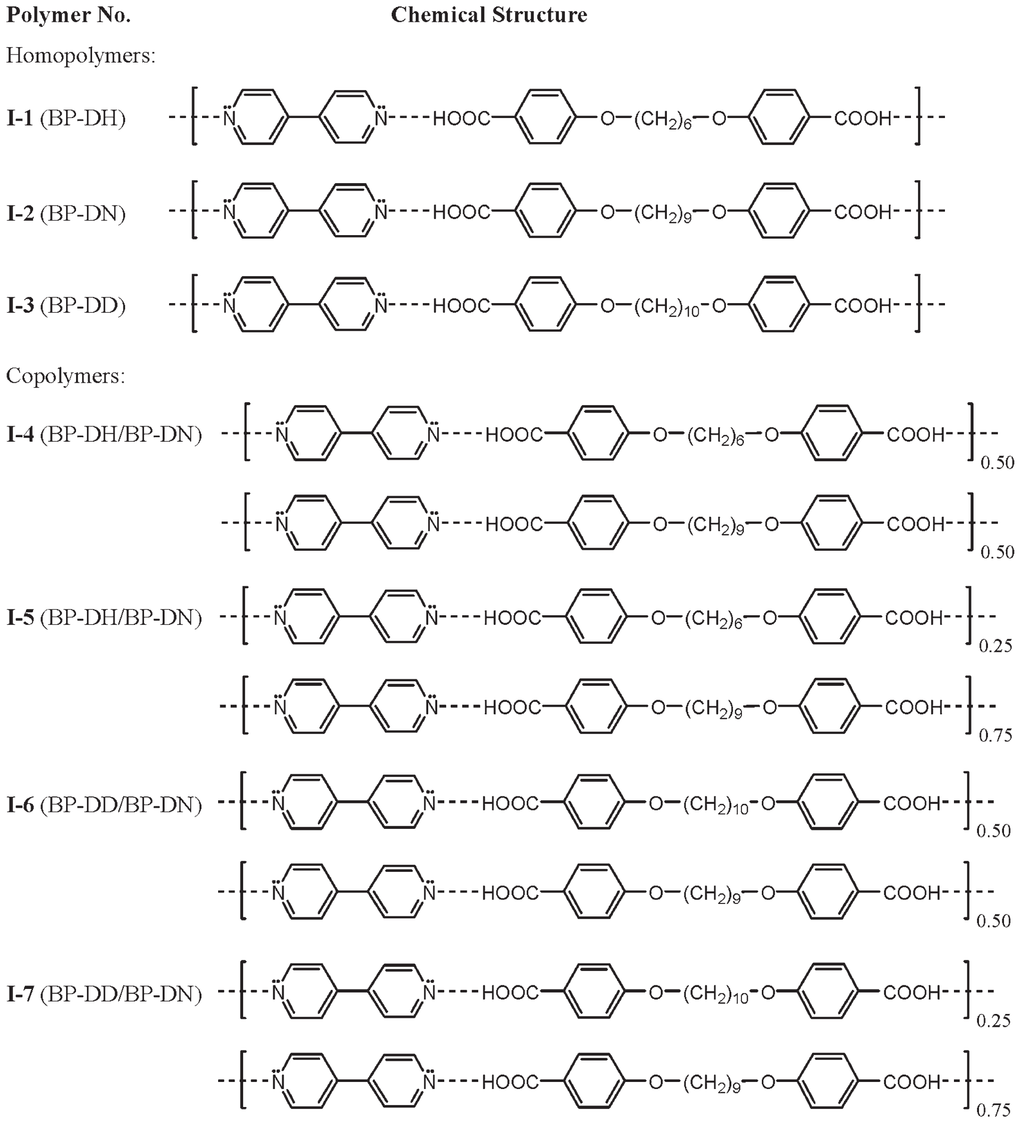

Scheme 1. Polymer structures.

although at considerably higher temperatures. The formation of both supramolecular polymers and their LC phases derives directly from the H-bond association. We also reported the preparation and characterization of chain-extended supramolecular polymers of 4,4′-bipyridyl with adipic and/or sebacic acids, which exhibit thermotropic LC properties. They typically exhibit smectic phases, and even copolymers, unlike many other thermotropic LCPs, also exhibit smectic phases [48, 49].

In this article, we describe the preparation and characterization of chain-extended supramolecular polymers of 4,4′-bipyridyl with various 4,4′-dicarboxy-α,ω-diphenoxyalkanes. These benzoic acid derivatives are selected for the preparation of the polymers, since they are conducive to the formation of an LC phase because of the presence of aromatic moieties when compared with aliphatic dicarboxylic acids [50]. Several main chain supramolecular polymers that exhibit thermotropic LC properties have been reported based on a benzoic acid derivative containing oxyethylene groups [41–47]. The narrow temperature range of LC or monotropic phases in these supramolecular polymers is related to the presence of flexible oxyethylene groups. Thus, supramolecular polymers based on benzoic acid derivatives containing variable methylene units are of considerable interest in the development of this class of polymers having a broad LC phase range. The methylene units selected for the benzoic acid derivatives are 6, 9 and 10 so that one can examine the odd–even effect on the thermal properties of the polymers.

We note that the induction of liquid crystallinity via the H-bond is limited to a large extent to side chain LCPs [21, 27, 51–53], but relatively few studies have been reported for main chain LCPs through the

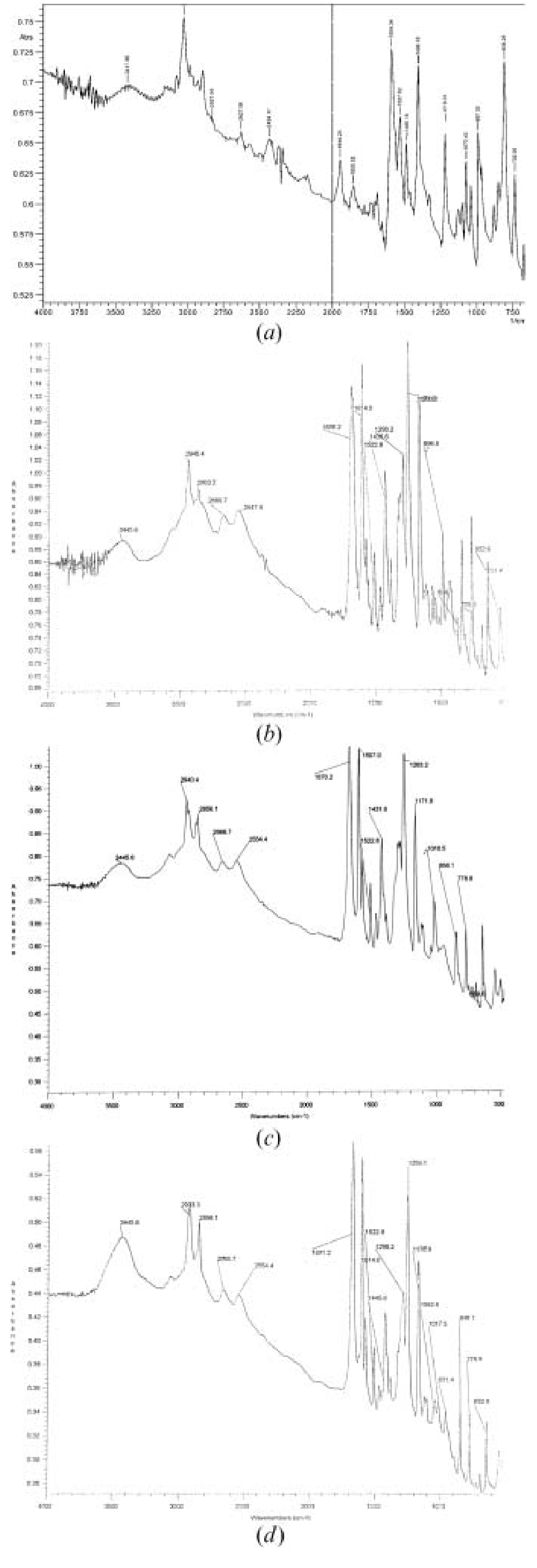

Figure 1. FTIR spectra of (a) 4,4′-bipyridyl, (b) DH, (c) DN and (d) DD taken at room temperature.

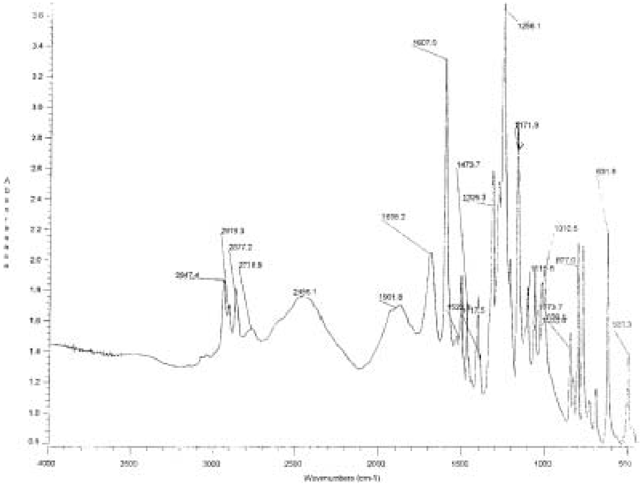

Figure 2. FTIR spectrum of polymer **I-1** taken at room temperature.

Table 1. Characteristic IR absorption bands of polymers prepared from 4,4′-bipyridyl and 4,4′-dicarboxy-α,ω-diphenoxyalkanes.

Polymer	Monomer[a]	New O–H bands in N---H–O/cm^{-1}	C=O band/cm^{-1}	O---H–O OOP wagging/cm^{-1}
I-1	BP+DH	2449, 1890	1692	
I-2	BP+DN	2493, 1894	1685	
I-3	BP+DD	2459, 1893	1691	
I-4	BP+DH+DN (0.50)	2455, 1904	1692	
I-5	BP+DH+DN (0.75)	2465, 1908	1692	
I-6	BP+DD+DN (0.50)	2461, 1893	1695	
I-7	BP+DD+DN (0.75)	2458, 1897	1694	
	DH		1685	947
	DN		1677	950
	DD		1677	964

[a] BP=4,4′-bipyridyl; DH=4,4′-dicarboxy-1,6-diphenoxyhexane; DN=4,4′-dicarboxy-1,9-diphenoxynonane; DD=4,4′-dicarboxy-1,10-diphenoxydecane.

secondary interactions of H-bonds [33, 41–49, 54]. Therefore, it was of principal interest to study the thermotropic LC properties of new, chain-extended, supramolecular polymers that derive directly from these secondary interactions and to understand the structure–property relationships of this novel class of polymers. The effects of copolymerization on both the thermal transitions and the nature of LC phases for these polymers were also examined. The structures and designations of these supramolecular polymers (**I**), which were prepared and characterized, are shown in scheme 1. They were all characterized for their thermotropic properties by a number of experimental techniques, including Fourier transform infrared (FTIR), DSC, POM and thermogravimetric analysis (TGA).

2. Experimental

2.1. *Monomer synthesis*

4,4′-Bipyridyl was purchased from Tokyo Kasei Kogyo Co., Ltd., and purified by recrystallization twice from toluene, giving a melting point of 112–114°C. The three proton donors used were 4,4′-dicarboxy-1,6-diphenoxyhexane (DH), 4,4′-dicarboxy-1,9-diphenoxynonane (DN) and 4,4′-dicarboxy-1,10-diphenoxydecane (DD). They were prepared by the reaction of 4-hydroxybenzoic acid with the corresponding α,ω-dibromoalkanes according to the previously reported procedure [55]. The first diacid was recrystallized from *N*,*N*-dimethylformamide (DMF)/95% ethanol, the second and third diacids were purified by recrystallization of their dipotassium salts from aqueous ethanol and followed by acidification; melting points were 304–307°C (298–300°C [56]), 258–262°C (255–258°C [55]) and 275–279°C (276–278°C [56]), respectively, as determined by DSC at a heating rate of 10°C min^{-1}. Each of the two diacids (DH and DN) also exhibited a crystal-to-crystal transition at low temperature before the melting transition.

2.2. *Polymer synthesis*

All of the polymers in this study were prepared by the slow evaporation technique [57] from a pyridine solution containing equimolar amounts of 4,4′-bipyridyl and the corresponding 4,4′-dicarboxy-α,ω-diphenoxyalkanes or a mixture of 4,4′-dicarboxy-α,ω-diphenoxyalkanes of various compositions; this was followed by drying *in vacuo* at 50°C for 24 h.

2.3. *Polymer characterization*

IR spectra were recorded with a Nicolet FTIR analyser with neat films of polymers on KBr pellets. Phase transition temperatures were measured with a TA DSC 910 with a Thermal Analyzer 2100 system, calibrated with indium and tin, under a nitrogen flow at heating and cooling rates of 10°C min^{-1}, unless otherwise specified. The peak maxima of the endotherms were taken as the transition temperatures. The LC texture of each of the polymers was observed by POM using a Nikon Labophot 2 microscope equipped with crossed polarizers and a Mettler hot stage. TGA was performed with a TA Instruments analyser 2100 system at a heating rate of either 10 or 20°C min^{-1} under a nitrogen flow.

3. Results and discussion

Figure 1 shows the FTIR spectra of the hydrogen-bonded acceptor and donors taken at room temperature, which may be compared with those of hydrogen-bonded polymers made from these precursors.

Figure 2 shows the IR spectrum of H-bonded polymer **I-1** taken at room temperature. The appearance of new –OH bands at 2449 and 1890 cm^{-1}, and the disappearance of the out-of-plane (OOP) H–O–H wagging vibration band of carboxylic acid dimer at 947 cm^{-1}, indicate the presence of strong hydrogen bonding between the –OH group of –COOH and the pyridyl nitrogen of 4,4′-bipyridyl, which is in good agreement with the reported results of other similar H-bonded polymers [58].

However, the carbonyl band centred at 1692 cm^{-1} in the polymer is slightly shifted to higher wavenumber in comparison with that of DH dimer. This result is in good agreement with the shifting of the carbonyl band of the H-bonded complex, which is prepared from bispyridyl and benzoic acid derivative, to higher wavenumber in comparison with that of the benzoic acid dimer, because of complexation between the two components through hydrogen bonds. Similarly, other polymers (**I-2** to **I-7**) exhibited qualitatively identical absorption bands to those of polymer **I-1**. Their characteristic absorption bands, including those of DH, DN and DD for comparison, are collected in table 1.

Although both the H-bond acceptor (4,4′-bipyridyl) and the H-bond donors (DH, DN and DD) exhibited no LC properties and have melting points at 304–307, 258–262, and 275–279°C, respectively, LC phases were observed in each of the H-bonded polymers, including copolymers that were prepared from the donor and acceptor components. The DSC thermograms of the H-bond acceptor and the H-bond donors are shown in figure 3 and may be compared with those of the H-bonded polymers.

The DSC thermograms of polymer **I-1** are shown in figure 4. Its thermogram in the first heating cycle showed three distinct endotherms at 219, 237 and 254°C. In the subsequent cooling cycle, there were three corresponding exotherms at 170, 216 and 247°C, respectively. Similarly, three endotherms and three exotherms were observed in the second heating and cooling cycles. The minor differences between successive heating and cooling cycles were as follows. The peak maxima of endotherms in the first heating and cooling cycles were slightly shifted to higher temperatures in the second heating and cooling cycles. The enthalpy changes for all of the transitions in the second heating and cooling cycles decreased significantly, in comparison with those of the corresponding transitions in the first heating and cooling cycles, with the exception of the recrystallization exotherm in the second cooling cycle, which was slightly increased in comparison with that in the first cooling cycle. The degrees of supercooling of these endothermic transitions were 49, 21 and 7°C in the first cooling cycle, respectively. Similar degrees of supercooling for these transitions were also observed in the second cooling cycle.

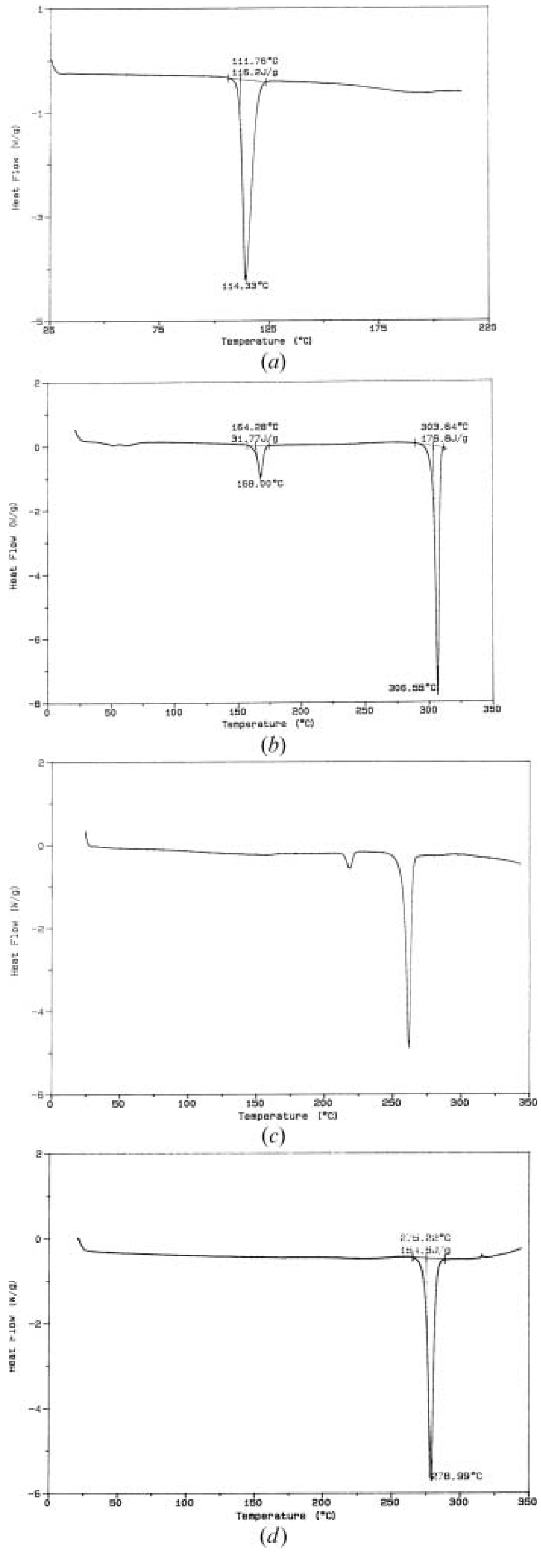

Figure 3. DSC thermograms of (a) 4,4′-bipyridyl, (b) DH, (c) DN and (d) DD, obtained at a heating rate of 10°C min^{-1}.

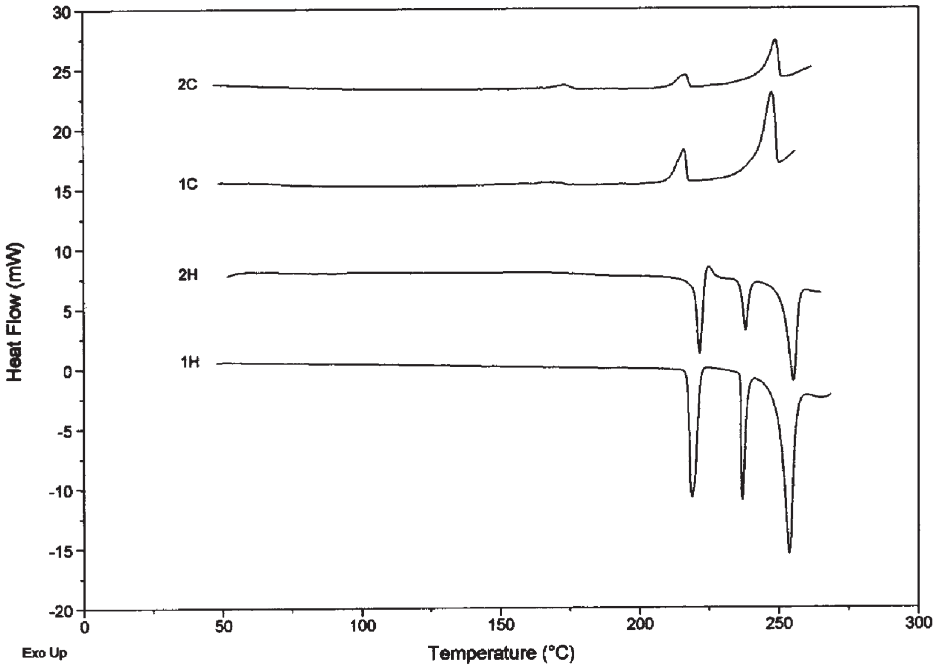

Figure 4. DSC thermograms of polymer **I-1** obtained at heating and cooling rates of 10°C min^{-1}.

POM studies suggested that the lowest temperature endotherm corresponded to the crystal-to-LC phase transition (T_m), which underwent an appreciable degree of supercooling, as expected [59]. The other two high temperature endotherms were presumably related to transitions of the high-order smectic to the low-order smectic phase. The exact nature of these transitions could not be determined due to the viscous nature of the melt. Surprisingly, the intermediate endotherm had a higher degree of supercooling (21°C) than the highest temperature endotherm (6 or 7°C); this was in marked contrast to those of thermotropic LCPs [60–62].

No smectic-to-isotropic transition (T_i) was detected for polymer **I-1** up to the decomposition temperature. Usually, the T_m of an LCP exhibits a high degree of supercooling, but the LC-to-LC transition or T_i exhibits characteristically little or no supercooling. In fact, the degrees of supercooling of various thermal transitions of an LCP in the DSC thermograms can be used for the identification of T_m, $T_{LC/LC'}$ and T_i [59–62].

The DSC thermograms of polymer **I-2**, shown in figure 5, exhibited three endotherms at 205, 223 and 230°C in the first heating cycle. Correspondingly, there were three exotherms at 146, 212 and 222°C in the first cooling cycle. The intermediate endotherm appeared as a shoulder of the highest temperature endotherm. During the first cooling cycle, the degrees of supercooling were 59, 11 and 8°C, respectively. However, there were four endotherms at 183, 205, 228 and 233°C in the second heating cycle and also four exotherms at 147, 201, 213 and 224°C in the second cooling cycle. The degrees of supercooling in the second cooling cycle were 46, 4, 15 and 9°C, respectively. The highest temperature endotherm in the second heating cycle had a shoulder similar to the highest temperature endotherm in the first heating cycle. The highest degree of supercooling for the lowest temperature endotherm indicated that this transition was related to T_m at 205°C, which was confirmed by POM studies. These studies also suggested that the highest temperature endotherm corresponded to T_i at 230°C, which was expected because of the odd–even effect [63]. The highest enthalpy change as high as 55.6 kJ mol^{-1} for this transition also indicated its T_i. As for polymer **I-1**, the enthalpy change for the low-temperature endotherm was much smaller than that for the high-temperature endotherm.

The DSC thermograms of polymer **I-3** are shown in figure 6. There were three endotherms at 219, 238 and 248°C in the first heating cycle, and three corresponding exotherms at 204, 228 and 239°C in the first cooling cycle. The highest temperature endotherm at 248°C appeared as a shoulder of the endotherm at 238°C. In contrast, there were two endotherms at 226 and 241°C in the second heating cycle, and two corresponding exotherms at 207 and 232°C in the second cooling cycle. The endothermic and exothermic peak maxima in the second heating and cooling cycles were shifted to higher temperatures in comparison with those in the first heating and cooling cycles. The enthalpy changes for all of these transitions in the second heating and cooling

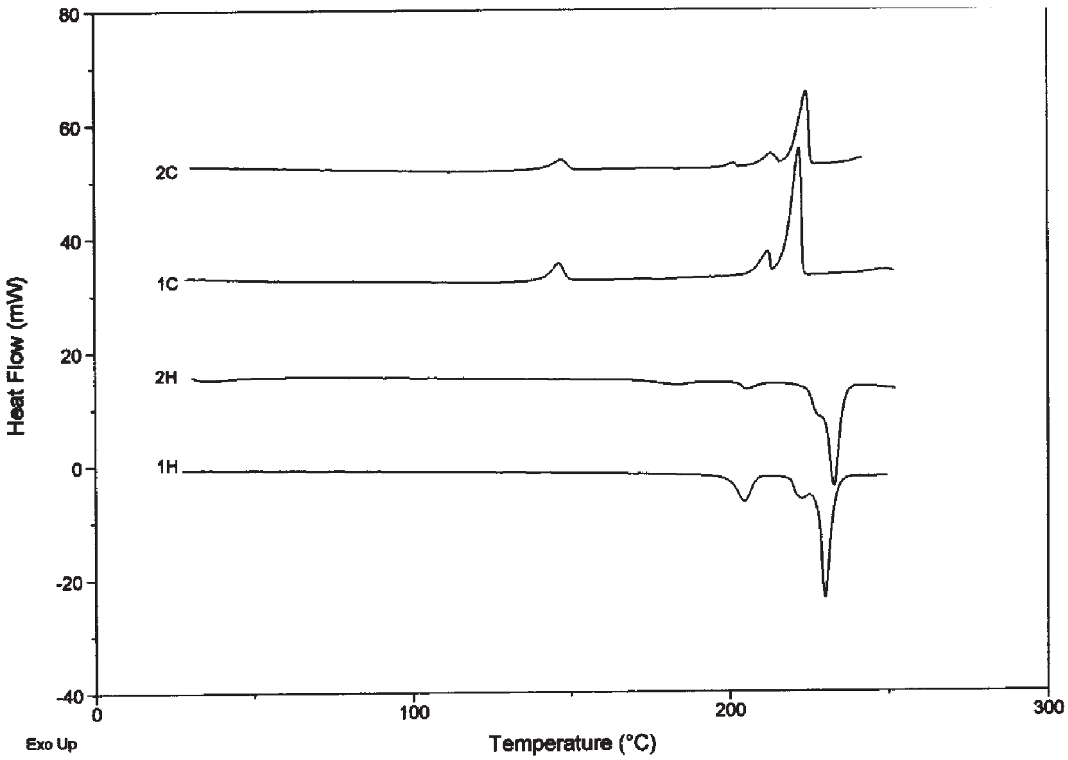

Figure 5. DSC thermograms of polymer **I-2** obtained at heating and cooling rates of 10°C min^{-1}.

cycles decreased significantly in comparison with those in the first heating and cooling cycles. The degrees of supercooling of the endothermic transitions in the first heating cycle were 16, 10 and 9°C, respectively; those of endothermic transitions in the second heating cycle were 19 and 9°C, respectively. As for polymer **I-1**, the lowest

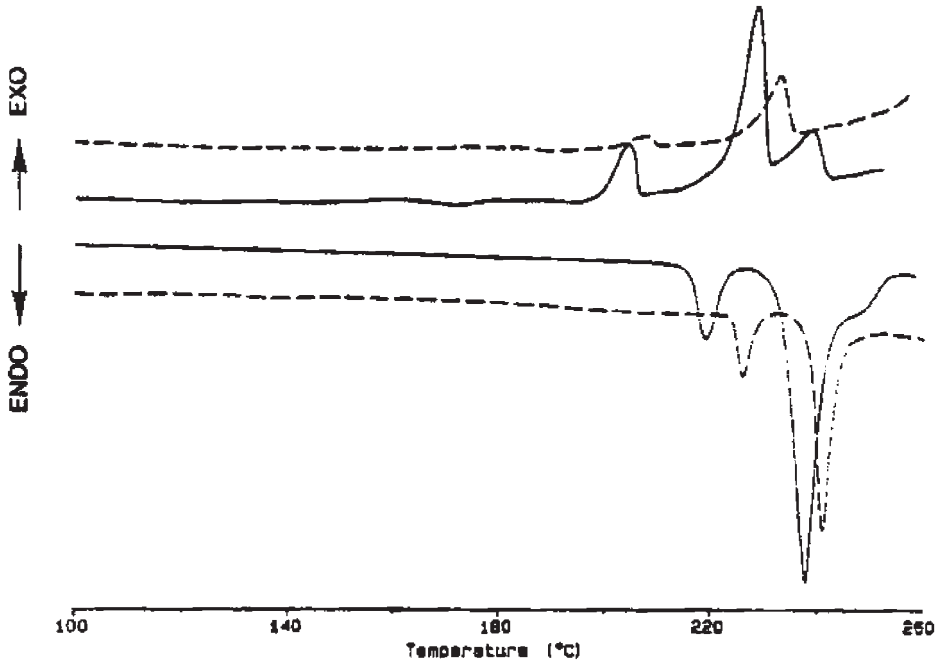

Figure 6. DSC thermograms of polymer **I-3** obtained at heating and cooling rates of 10°C min^{-1}: — (1H, 1C) and --- (2H, 2C).

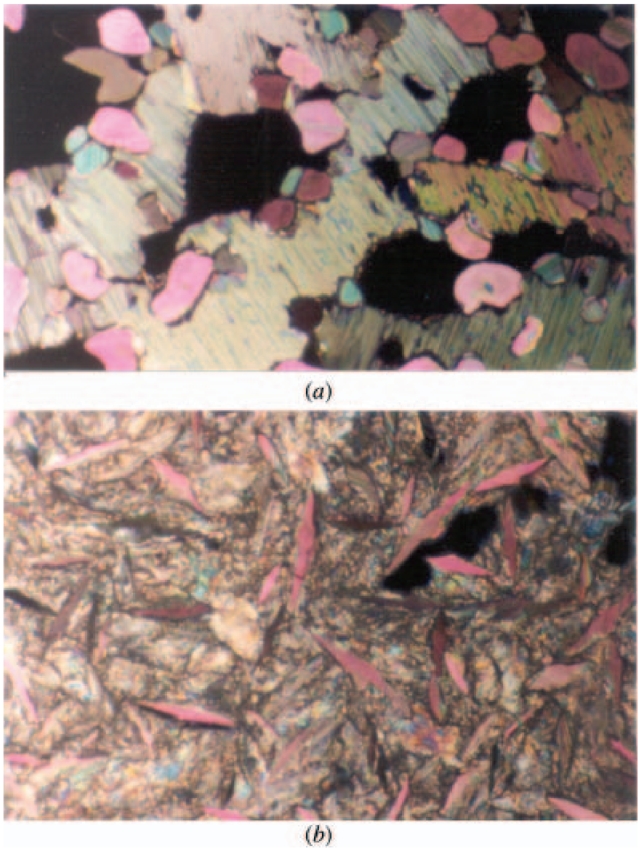

Figure 7. Photomicrographs of polymer **I-2**: (a) taken at 150°C after cooling at 10°C min^{-1} from the isotropic phase displaying a mosaic texture; (b) taken at room temperature after cooling at 10°C min^{-1} from the isotropic phase displaying a bâtonnets texture (magnification 400 ×).

temperature endotherm was related to T_{m}, which underwent a high degree of supercooling [59–62]. Additionally, no T_{i} was observed for polymer **I-3**, as for polymer **I-1**, up to the decomposition temperature, which was verified by POM studies.

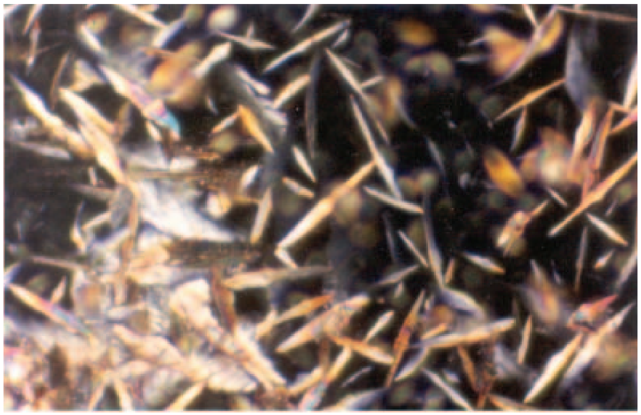

Figure 8. Photomicrograph of polymer **I-3** taken at room temperature on cooling rapidly from 250°C, displaying a bâtonnets texture (magnification 400 ×).

A photomicrograph of polymer **I-2** taken at 150°C after it was cooled from the isotropic phase at a rate of 10°C min^{-1} is shown in figure 7 a; a mosaic texture is seen, indicative of its high-order smectic phase, which includes SmB, SmE, SmF, SmG and SmI phases. The texture exhibits various regions with uniform director patterns. In many cases, the mosaic texture of an LC polymer can retain to a large extent the texture of the preceding high-temperature smectic phases, such as SmA or SmC [64]. For example, figure 7 b shows a photomicrograph of polymer **I-2**, taken on cooling from the isotropic phase to room temperature, displaying a texture that consists of long bâtonnets indicative of high-temperature SmA or SmC.

Although neither polymers **I-1** and **I-3** exhibited isotropic transitions, on cooling from high temperature to room temperature each showed a long bâtonnets texture (figure 8), which indicated that their high temperature transitions were related to the formation of low-order smectic phases. However, both the T_{m} and T_{i} of polymer **I-2** were lower than those of polymers **I-1** and **I-3** as expected, and these results were presumably due to the presence of nine (odd number) methylene units present in the former in comparison with the six and ten (even number) methylene units in the latter [63]. These results are in good agreement with the reported results for other semiflexible thermotropic LCPs [60–62].

The enthalpy change of isotropization (ΔH_{i}) of polymer **I-2** (table 2) was quite high, suggesting that this polymer had an increased flexibility in the isotropic phase with respect to its smectic phase. These results are also in agreement with those for other semiflexible thermotropic LCPs reported by Chiellini and coworkers [65]. The LC phase range ($T_{\mathrm{i}}-T_{\mathrm{m}}$) for this H-bonded polymer **I-2** were 25 and 28°C in the first and second heating cycles, respectively, which were quite broad.

Both the polymers **I-1** and **I-3** exhibited LC phases until their decomposition temperatures. Interestingly, the LC phase range for each was much higher than those (5.3 and 4°C) of H-bonded polymers of *trans*-1,2-bis(4-pyridyl)ethylene (as a H-bond acceptor) with tetraethyleneglycoxybis(4-benzoic acid) or pentaethyleneglyoxybis(4-benzoic acid) (as H-bond donors), respectively [43, 44]. The mesogenic (LC forming unit) in each of these homopolymers consists of the 4,4′-bipyridyl moiety hydrogen bonded with the carboxyl groups of DH, DN and DD components. In contrast, the mesogenic units in the latter complexes are extended aromatic rod-like units composed of *trans*-1,2-bis(4-pyridyl)ethylene hydrogen bonded with derivatives of

Table 2. Thermal properties of H-bonded polymers prepared from 4,4′-bipyridyl and 4,4′-dicarboxy-α,ω-diphenoxyalkanes: transition temperatures (°C) and enthalpies (kJ mol^{-1}, in parentheses).

Polymer	Monomer[a]		T_m	$T_{LC/LC'}$	$T_{LC'/LC''}$	$T_{LC''/LC'''}$	T_i	ΔT
I-1	BP+DH	1H[b]	219 (18.5)	237 (10.2)	254 (34.2)			
		1C	170 (0.7)	216 (5.8)	247 (17.2)			
		2H	222 (12.8)	240 (5.5)	255 (18.0)			
		2C	173 (1.0)	217 (2.7)	249 (8.4)			
I-2	BP+DN	1H	205 (16.2)	223 (10.3)			230 (55.6)	25
		1C	146 (9.1)	212 (9.8)			222 (52.8)	
		2H	83, 205 (3.2), (3.1)	228 (9.9)			233 (32.5)	28
		2C	147, 201 (5.8), (1.2)	213 (6.3)			224 (32.5)	
I-3	BP+DD	1H	219 (9.9)	238 (48.7)	248 (13.7)			
		1C	204 (6.7)	228 (27.6)	239 (7.8)			
		2H	226 (5.8)	241 (25.1)				
		2C	207 (1.4)	232 (9.2)				
I-4	BP+DH+DN (0.50)	1H	194 (2.9)	216	222	238		
		1C	171 (5.5)	195 (1.5)	206 (24.7)	213 (4.4)		
		2H		216		239		
		2C	171 (4.5)	194 (1.6)	208 (21.8)	214 (2.7)		
I-5	BP+DH+DN (0.75)	1H	192 (12.8)				214 (80.5)	22
		1C	197 (17.7)	204 (44.2)			212 (15.1)	
		2H					217 (75.4)	
		2C	201 (18.5)	207 (41.7)			215 (12.6)	
I-6	BP+DD+DN (0.50)	1H		216 (9.1)			231 (71.2)	
		1C		204 (7.9)			222 (61.1)	
		2H	191 (0.6)	218 (8.7)			229 (51.3)	38
		2C	171 (1.2)	203 (5.0)			222 (37.0)	
I-7	BP+DD+DN (0.75)	1H		216 (13.5)			227 (78.7)	
		1C	97 (1.4)	206 (9.4)			219 (74.9)	
		2H	151 (5.1)	219 (12.8)			228 (74.6)	77
		2C	97 (0.8)	207 (8.7)			220 (71.1)	

[a] See the footnote in table 1 for definitions of BP, DH, DN and DD. [b] 1H(C) denotes first heating (cooling), etc.

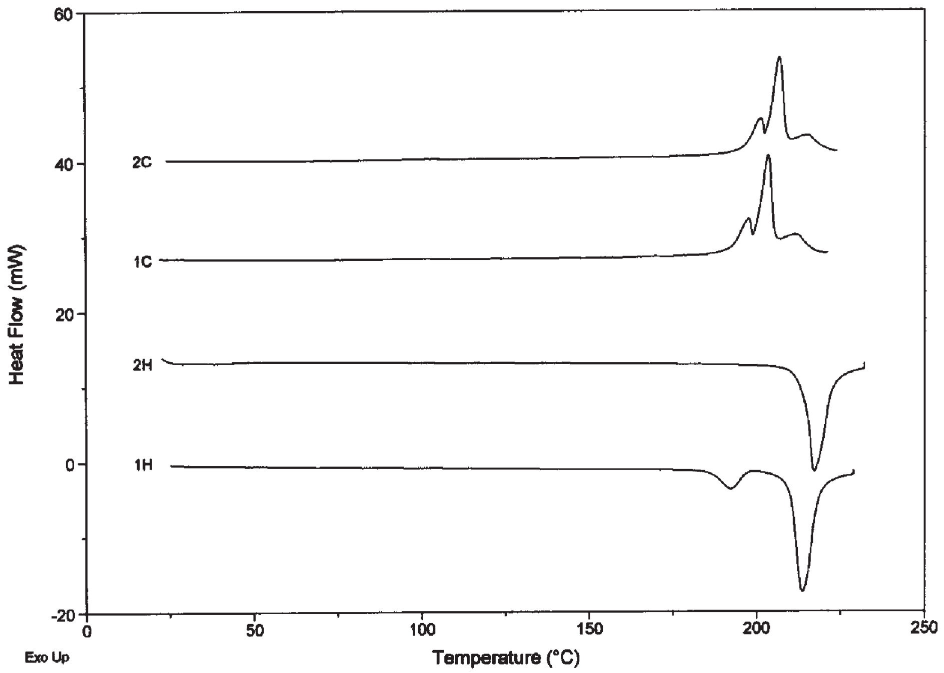

Figure 9. DSC thermograms of polymer **I-5** obtained at heating and cooling rates of 10°C min^{-1}.

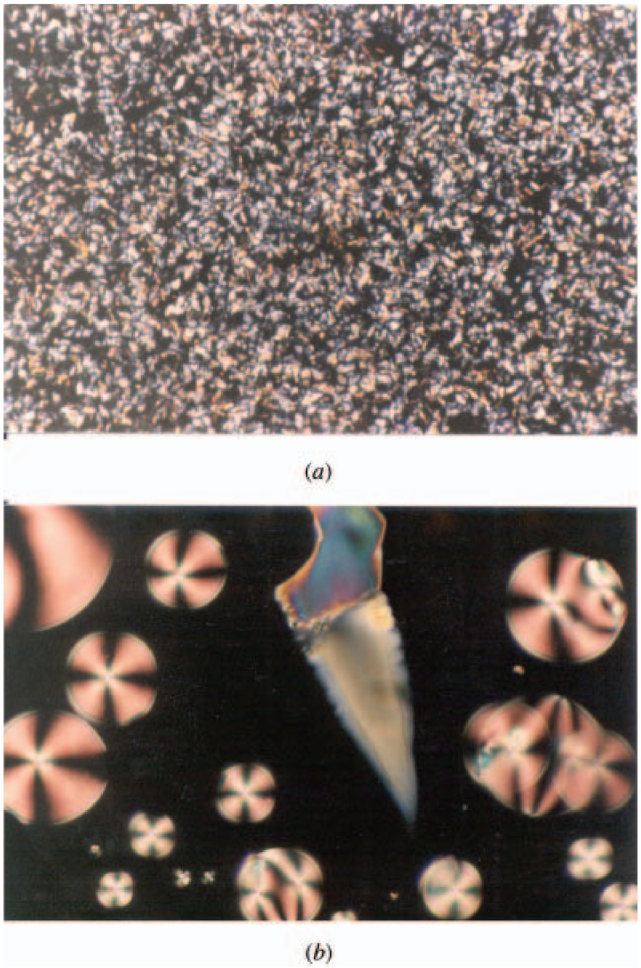
(a)

(b)

Figure 10. Photomicrographs of (a) polymer **I-4** taken at 240°C displaying a bâtonnets texture, and (b) polymer **I-5** taken at 210°C on cooling from the isotropic phase, displaying a schlieren texture with only four brushes (magnification 400 ×).

the bis(4-benzoic acid) moiety from the H-bonded donor components. Therefore, the observation of smectic phases in these homopolymers was quite significant in the sense that the 4,4′-bipyridyl unit complexed with the carboxyl groups of DH, DN and DD could exceed the axial ratio limit (a measure of mesogenicity for a rod-like unit) for the formation of an LC phase. Additionally, the formation of smectic phases in both heating and cooling cycles, i.e. enantiotropic LC phases for these polymers as opposed to SmA formation in the cooling cycle only for the polymer of *trans*-1,2-bis(4-pyridyl)ethylene with tetraethyleneglycoxybis(4-benzoic acid) and to SmA formation in the second heating cycle for the polymer of *trans*-1,2-bis(4-pyridyl)ethylene with pentaethyleneglycoxybis(4-benzoic acid) [43, 44], presumably occurred for two reasons. These are (a) the high polarizability, i.e. high electron density, of the 4,4′-bipyridyl moiety H-bonded with DH, DN and DD in comparison with that of *trans*-1,2-bis(4-pyridyl)ethylene H-bonded with tetraethyleneglycoxybis(4-benzoic acid) and pentaethyleneglycoxybis(4-benzoic acid); and (b) the greater flexibility of oxyethylene units in comparison with the methylene units.

Copolymer **I-4**, prepared from 4,4′-bipyridyl and a mixture of DH and DN (50/50), showed four endotherms in the first DSC heating cycle. Correspondingly, there were four exotherms in the first cooling cycle. However, only two endotherms were seen in the second heating cycle. In the subsequent second cooling cycle, there were four exotherms as in the first cooling cycle (not shown). The lowest temperature endotherm at 194°C was related to T_m, and no T_i was observed for this copolymer as determined in conjunction with POM studies. Copolymer **I-5**, prepared from 4,4′-bipyridyl and a mixture of DH and DN (25/75), exhibited two endotherms in the first DSC heating cycle, but three exotherms in the first cooling cycle. It exhibited a single endotherm in the second heating cycle, but three exotherms in the second cooling cycle as in the first cooling cycle (figure 9). The two endotherms at 192 and 214°C were identified in conjunction with POM as T_m and T_i transitions, respectively, giving an LC phase range of 22°C. Figure 10 shows photomicrographs of polymers **I-4** and **I-5** taken at 240 and 210°C, respectively, displaying distinctly their smectic LC phases [66–68].

Copolymer **I-6**, prepared from 4,4′-bipyridyl and a mixture of DD and DN (50/50), did not exhibit a T_m in the first heating cycle and, correspondingly, there was no exotherm in the first cooling cycle. Similarly, copolymer **I-7**, prepared from 4,4′-bipyridyl and a mixture of DD and DN (25/75), did not exhibit a T_m in the first heating cycle but showed an additional exotherm at the lowest temperature, which was confirmed by POM. However, both copolymers exhibited three endotherms in their second heating cycles and three corresponding exotherms on second cooling. The DSC thermograms of copolymer **I-7** obtained at heating and cooling rates of 10°C min^{-1} are shown in figure 11. The degrees of supercooling in the second heating cycle were 20, 15 and 7°C for copolymer **I-6** and 54, 12 and 8°C for copolymer **I-7**. These results suggest that the lowest temperature endotherms, at 191°C for copolymer **I-6** and at 151°C for copolymer **I-7**, were related to their T_m transitions, and the highest temperature endotherms at 229 and 228°C, respectively, were related to their T_i transitions; this was confirmed by POM studies.

Figure 12 shows photomicrographs of polymers **I-6** and **I-7** taken at room temperature on cooling from the isotropic phase; they display high-order smectic phases.

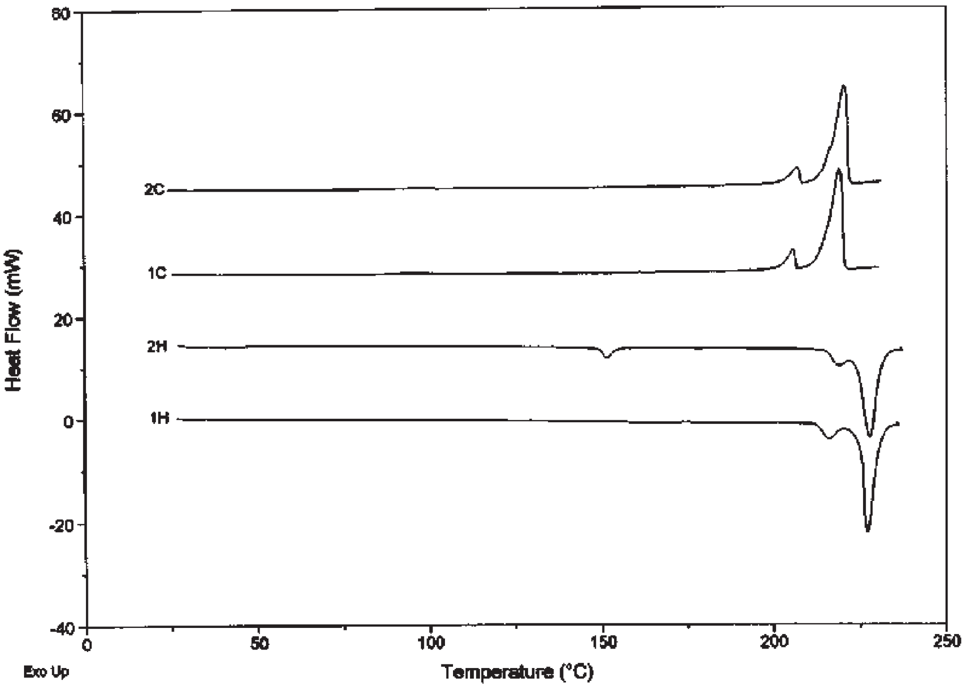

Figure 11. DSC thermograms of polymer **I-7** obtained at heating and cooling rates of 10°C min^{-1}.

In figure 10 a, the schlieren texture of a low-order smectic phase was clearly visible along with the mosaic texture of a high-order smectic phase, even at room temperature [64, 66–68]. For both these copolymers, the enthalpy changes for all the transitions in the second heating and cooling cycles were lower than those of the corresponding transitions in the first heating and cooling cycles. The large enthalpy changes for T_i transitions in the first heating cycles were 71.2 and 78.7 kJ mol^{-1}, respectively, suggesting their smectic-to-isotropic transitions. In comparison with homopolymers **I-1** to **I-3**, the transition temperatures of copolymers **I-6** and **I-7** were shifted to lower temperatures and consequently their T_i transitions were also observed without the interference of their thermal decomposition.

The thermal transitions determined by DSC and their associated thermodynamics parameters for polymers **I-1** to **I-7** are collected in table 2. The ΔH_i values at T_i transitions for polymers **I-2** and **I-5** to **I-7** in their first heating cycles were particularly high and in the range 55.6–80.5 kJ mol^{-1} per repeating unit. In general, ΔH_i values at T_i transitions for many semiflexible thermotropic LCPs are in the range 1.3–3.6 kJ mol^{-1} per repeating unit for a nematic LC phase and 6.3–20.9 kJ mol^{-1} per repeating unit for smectic LC phases, depending on the type or order of the smectic phase [69]. As expected, the T_m values of the copolymers were lower than those of the respective homopolymers because of the copolymerization effect of DH, DN and DD in the copolymer chains, and are in good agreement with the results for many thermotropic semiflexible LCPs [60–62]. Additionally, the T_i values of copolymers **I-5** and **I-7** were slightly lower than that of homopolymer **I-2**, but the T_i value of copolymer **I-6** was essentially identical to that of homopolymer **I-2**. Consequently, their LC phase ranges ($\Delta T = T_i - T_m$) were higher than those of the respective homopolymer **I-2**, with the exception that copolymer **I-5** had a slightly reduced LC phase range.

Each of the polymers underwent crystallization on cooling at a rate of 10°C min^{-1} from the smectic or isotropic phase, which was confirmed by the fact that each had a crystallization exotherm in each cooling cycle. All of the polymers **I-1** to **I-7**, including the copolymers, showed two smectic phases of both high order and low order; this phenomenon is commonly called polymesomorphism. Generally, it occurs in monomeric liquid crystals (MLCs), but rarely in thermotropic LCPs. As a consequence of high molecular weight of an LCP, the number of LC phases through which a polymer passes is fewer than for an MLC. Often, only one LC phase exists for an LCP [70]. In contrast, the polymers in the present study showed a high-order smectic phase that includes SmB, SmE, SmF, SmG and SmI phases and low-order smectic phases (SmA or SmC). The exact nature of both low-order and high-order smectic phases must be determined by X-ray analyses at variable temperatures. It is

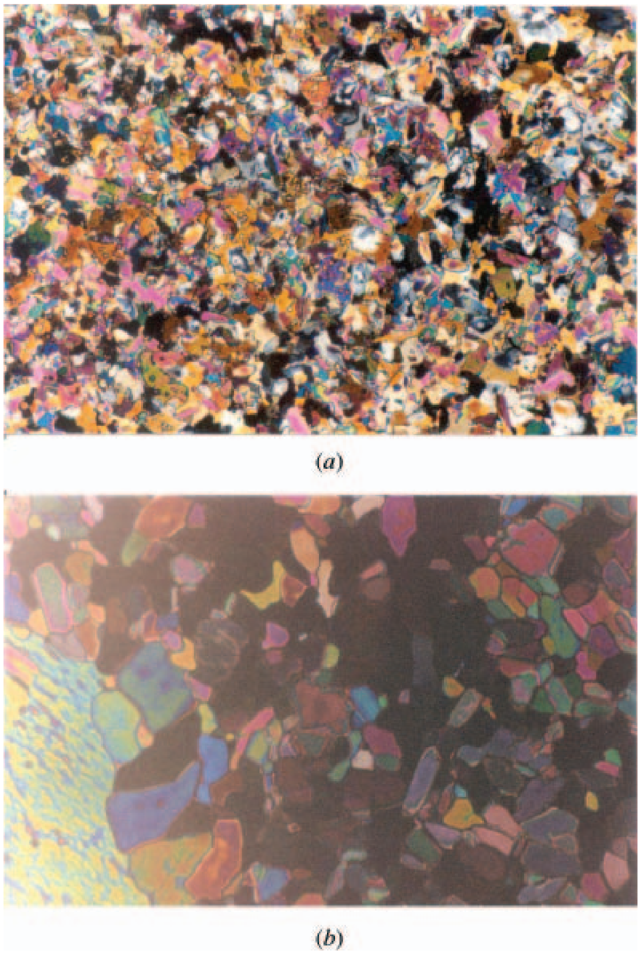
(*a*)

(*b*)

Figure 12. Photomicrographs of (a) copolymer **I-6** taken at room temperature on cooling from the isotropic phase, displaying a mosaic texture; (b) polymer **I-7** taken at 215°C on cooling at a rate of $10^\circ\mathrm{C\,min^{-1}}$ from the isotropic phase, displaying a mosaic texture (magnification 400 ×).

relevant to mention here that, in the field of thermotropic LCPs, copolymerization usually suppresses the formation of a smectic phase and promotes the formation of a nematic phase [71]. This phenomenon was not observed in these H-bonded polymers, suggesting that the 4,4′-bipyridyl moiety, connected through the H-bond with derivatives of bis(4-benzoic acid) such as DH, DN and DD, acted as a strong smectogenic unit for the preparation of main chain H-boned polymers.

The thermal stability [decomposition temperature (T_d)] of each of the polymers was determined in nitrogen by TGA. The thermal stability limit was taken as the temperature in °C at which a 5% weight loss occurred. Figure 13 shows a typical TGA plot of polymer **I-2** in nitrogen obtained at a heating rate of $10^\circ\mathrm{C\,min^{-1}}$. Each of the homopolymers had a T_d value in the range 278–329°C at a heating rate of $10^\circ\mathrm{C\,min^{-1}}$. Each of the copolymers had T_d value in the range 254–356°C at a heating rate of $20^\circ\mathrm{C\,min^{-1}}$. Therefore, all of the thermal transitions for these polymers determined by DSC were well below their T_d values, allowing for the identification of the various LC phases occurring in these polymers.

4. Conclusions

A series of main chain, thermotropic, LC, hydrogen-bonded polymers was prepared by mixing 4,4′-bipyridyl as an H-bond acceptor and 4,4′-dicarboxy-α,ω-diphenoxyalkanes as H-bond donors from pyridine solution; their thermotropic LC properties were characterized by a number of experimental techniques. To our knowledge, they are the first examples of chain extended H-bonded main chain polymers containing 4,4′-dicarboxy-α,ω-diphenoxyalkanes as H-bond donors, which exhibit thermotropic LC properties. Some of them, including one homopolymer, exhibited enantiotropic smectic phase(s) having a broad LC phase range (22–77°C). Others exhibited enantiotropic smectic phases up to their decomposition temperatures. A majority of the previously reported main chain H-bonded polymers, prepared from bis(4-benzoic acid) derivatives such as [(oxydiethoxyethylene)dioxy]bis(4-benzoic acid) as H-bond donor and *trans*-1,2-bis(4-pyridyl)ethylene, 4,4′-(1,10-decanedioxy)diphenolbis(4-pyridinecarboxylate) and hydroquinonebis(4-pyridinecarboxylate) as H-bond acceptors, exhibit either monotropic SmA or nematic phase with a very narrow range [41–47].

We prepared four copolymers in this study to test the concept that copolymerization should disrupt the regularity of these H-bonded polymers required for the smectic-layered structure and, therefore, might lead to the formation of nematic phases. However, all the evidence indicated that these copolymers, like the homopolymers, exhibit only smectic phases. The anisotropic molecular shape of H-bonded 4,4′-bipyridyl moieties (which were built up from 4,4′-bipyridyl, DH, DN and DD components), and the attractive forces between these moieties, apparently stabilized smectic phases relative to the nematic phase. Furthermore, as for many thermotropic LCPs, copolymerization reduced T_m to a greater extent than T_i, resulting in a broad LC phase range for some of the copolymers. This had significant effect on controlling the thermal properties of supramolecular polymers that have become an exciting field of research. Therefore, it was found that the simple, single H-bond was capable of serving simultaneously both as the agent of liquid crystallinity and as the coupling bond generating an extended chain structure. This relatively new design concept represents a shift in emphasis from the

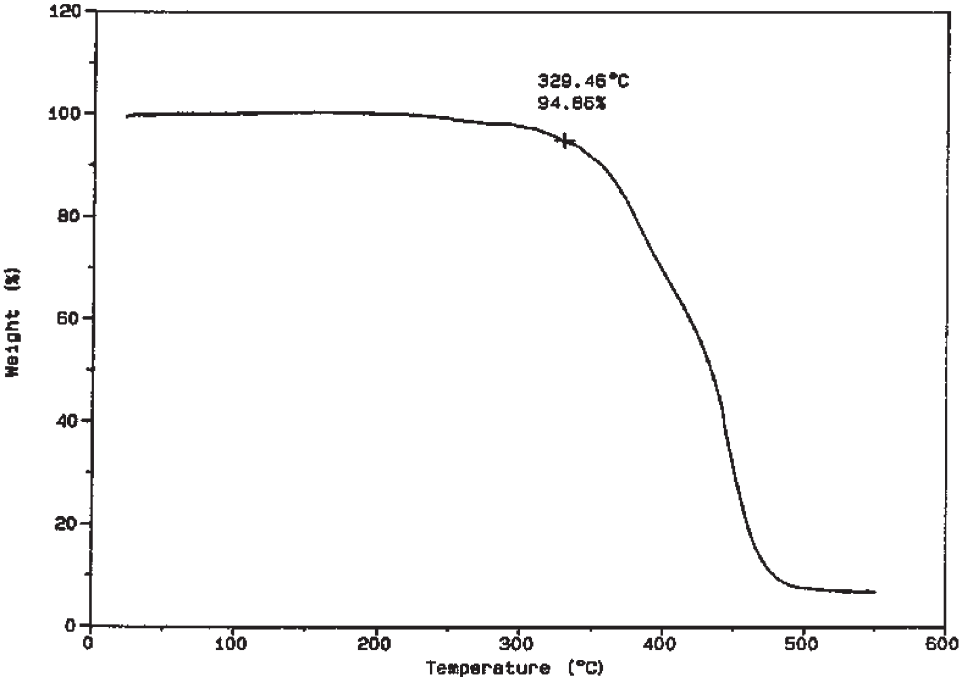

Figure 13. TGA plot of polymer **I-2** in nitrogen obtained at a heating rate of 10°C min^{-1}.

traditional approach of controlling properties by chemical synthesis and promises to yield a novel and important class of functional polymers. Such polymers containing components such as light- or electro-sensitive moieties and/or multiple binding may find applications in a wide range of electro-optic technologies or detection devices.

Acknowledgements

P. K. B. acknowledges the University of Nevada at Las Vegas (UNLV) for the startup, Stimulation, Implementation, Transition, and Enhancement (SITE), New Investigation Award (NIA) and Planning Initiative Award (PIA) grants; also the Donors of the Petroleum Research Fund (PRF), administered by the American Chemical Society, and an award from Research Corporation for the support of this research.

References

[1] R.P. Sijbesma, E.W. Meijer. *Chem. Commun.*, 5 (2003).

[2] J.-M. Lehn. *Polym. Int.*, **51**, 825 (2002).

[3] A.T. ten Cate, R.P. Sijbesma. *Macromol. Rapid Commun.*, **23**, 1095 (2002).

[4] V. Berl, M. Schmutz, M.J. Krische, R.G. Khoury, J.-M. Lehn. *Chem. Eur. J.*, **8**, 1227 (2002).

[5] L. Brunsveld, B.J.B. Folmer, E.W. Meijer, R.P. Sijbesma. *Chem. Rev.*, **101**, 4071 (2001).

[6] L.J. Prins, D.N. Reinhoudt, P. Timmerman. *Angew. Chem. Int. Ed.*, **40**, 2382 (2001).

[7] A. Ciferri (Ed.), *Supramolecular Polymers,* Chap. 1–15, Marcel Dekker, New York (2000).

[8] M. Fujita (Ed.), *Structure and Bonding Molecular Self-Assembly Organic Versus Inorganic Approaches,* Vol. 96, pp. 1–146, Springer-Verlag, Berlin (2000).

[9] D.N. Reinhoudt. *Supramolecular Materials and Technologies,* Vol. 4, Wiley, New York (1999).

[10] A.W. Bosman, H.M. Janssen, E.W. Meijer. *Chem. Rev.*, **99**, 1665 (1999).

[11] X.-D. Li, S.H. Goh. *J. Polym. Sci. B*, **41**, 789 (2003).

[12] X.-D. Li, S.H. Goh. *Polymer*, **43**, 6853 (2002).

[13] X.-D. Li, S.H. Goh. *J. appl. Polym. Sci.*, **81**, 907 (2001).

[14] M. Jiang, M. Li, M. Xiang, H. Zhou. *Adv. Polym. Sci.*, **146**, 121 (1999).

[15] X.-D. Huang, S.H. Goh, S.Y. Lee, Z.D. Zhao, M.W. Wong, C.H.A. Huan. *Macromolecules*, **32**, 4327 (1999).

[16] J.Y. Lee, P.C. Painter, M.M. Coleman. *Macromolecules*, **21**, 954 (1988).

[17] J.Y. Lee, P.C. Painter, M.M. Coleman. *Macromolecules*, **21**, 346 (1988).

[18] T. Kato. *Science*, **295**, 2414 (2002).

[19] C.M. Paleos, D. Tsiourvas. *Liq. Cryst.*, **28**, 1127 (2001).

[20] T. Kato, N. Mizoshita, K. Kanie. *Macromol. Rapid Commun.*, **22**, 797 (2001).

[21] G. Ambrožič, M. Žigon. *Macromol. Rapid Commun.*, **21**, 53 (2000).

[22] M. Lee, B.-K. Cho, Y.-K. Kang, W.-C. Zin. *Macromolecules*, **32**, 8531 (1999).

[23] A. Ciferri. *Liq. Cryst.*, **26**, 489 (1999).

[24] C.G. Bazuin. In *Mechanical and Thermophysical Properties of Polymer Liquid Crystals*, W. Brostow (Ed.), p. 59, Chapman & Hall, London (1998).

[25] A. Ciferri. *Trends Polym. Sci.*, **5**, 142 (1997).

[26] T. Kato. *Supramol. Sci.*, **3**, 53 (1996).

[27] T. Kato, J.M.J. Fréchet. *Macromol. Symp.*, **98**, 311 (1995).

[28] C.M. Paleos, D. Tsiourvas. *Angew. Chem. Int. Ed.*, **34**, 1696 (1995).

[29] V.V. Tsukruk, J.H. Wendorff. *Trends Polym. Sci.*, **3**, 82 (1995).

[30] C.T. Imrie. *Trends Polym. Sci.*, **3**, 22 (1995).

[31] J.-M. Lehn. *Angew. Chem. Int. Ed.*, **29**, 1304 (1990).

[32] C. Fouquey, J.-M. Lehn, A.-M. Levelut. *Adv. Mater.*, **2**, 254 (1990).

[33] J.-M. Lehn. *Makromol. Chem. Macromol. Symp.*, **69**, 1 (1993).

[34] M. Kotera, J.-M. Lehn, J.-P. Vigneron. *J. Chem. Soc., Chem. Commun.*, 197 (1994).

[35] A. Marsh, E.G. Nolen, K.M. Gardinier, J.-M. Lehn. *Tetrahedron Lett.*, **35**, 397 (1994).

[36] P.K. Bhowmik, H. Han, J.J. Cebe, R.A. Burchett, A.M. Sarker. *J. Polym. Sci. A*, **40**, 659 (2002).

[37] P.K. Bhowmik, H. Han, J.J. Cebe, R.A. Burchett. *J. Polym. Sci. A*, **40**, 141 (2002).

[38] D. Demus, J.W. Goodby, G.W. Gray, H.-W. Spiess, V. Vill (Eds). *Physical Properties of Liquid Crystals*, pp. 1–492, Wiley-VCH, Weinheim (1999).

[39] D. Demus, J.W. Goodby, G.W. Gray, H.-W. Spiess, V. Vill (Eds). *Handbook of Liquid Crystals,* Vol. 3, pp. 1–482, Wiley-VCH, Weinheim (1998).

[40] H. Han, P.K. Bhowmik. *Prog. Polym. Sci.*, **22**, 1431 (1997).

[41] C. He, A.M. Donald, A.C. Griffin, T. Waigh, A.H. Windle. *J. Polym. Sci. Part B*, **36**, 1617 (1998).

[42] C.-M. Lee, A.C. Griffin. *Macromol. Symp.*, **117**, 281 (1997).

[43] C. Alexander, C.P. Jariwala, C.-M. Lee, A.C. Griffin. *Macromol. Symp.*, **77**, 283 (1994).

[44] C.-M. Lee, C.P. Jariwala, A.C. Griffin. *Polymer*, **35**, 4550 (1994).

[45] P. Bladon, A.C. Griffin. *Macromolecules*, **26**, 6604 (1993).

[46] C. Alexander, C.P. Jariwala, C.-M. Lee, A.C. Griffin. *Polym. Prepr. (Am. chem. Soc., Div. polym. Chem.)*, **34**, 168 (1993).

[47] C. He, C.-M. Lee, A.C. Griffin, L. Bouteiller, N. Lacoudre, S. Boileau, C. Fouquey, J.-M. Lehn. *Mol. Cryst. liq. Cryst.*, **332**, 251 (1999).

[48] P.K. Bhowmik, X. Wang, H. Han. *J. Polym. Sci. A*, **41**, 1282 (2003).

[49] P.K. Bhowmik, X. Wang, H. Han. *Polym. Prepr. (Am. chem. Soc., Div. polym. Chem.)*, **36**, 124 (1995).

[50] L.J. Yu, J.S. Pan. *Liq. Cryst.*, **14**, 829 (1993).

[51] S. Malik, P.K. Dhal, R.A. Mashelkar. *Macromolecules*, **28**, 2159 (1995).

[52] T. Kato, Y. Kubota, T. Uryu, S. Ujiie. *Angew. Chem. Int. Ed.*, **36**, 1617 (1997).

[53] T. Kato, O. Ihata, S. Ujiie, M. Tokita, J. Watanabe. *Macromolecules*, **31**, 3551 (1998).

[54] P.K. Bhowmik, X. Wang, H. Han, A.M. Sarker. *Polym. Prepr. (Am. chem. Soc., Div. polym. Chem.)*, **36**, 324 (1995).

[55] H.B. Donahoe, L.E. Benjamin, L.V. Fennoy, D. Greiff. *J. Org. Chem.*, **26**, 474 (1961).

[56] A.-L. Liang, K.-Y. Hsu, C.-H. Li, T.-C. Chang. *Polymer*, **33**, 2217 (1992).

[57] T. Kato, A. Fujishima, J.M.J. Fréchet. *Chem. Lett.*, 919 (1990).

[58] T. Kato, J.M.J. Fréchet, P.G. Wilson, T. Saito, T. Uryu, A. Fujishima, C. Jin, F. Kaneuchi. *Chem. Mater.*, **5**, 1094 (1993).

[59] H. Han, P.K. Bhowmik, R.W. Lenz. *J. Polym. Sci. A*, **32**, 343 (1994).

[60] A.M. Donald, A.H. Windle. *Liquid Crystalline Polymers*, pp. 1–310, Cambridge University Press, Cambridge (1992).

[61] A. Ciferri (Ed). *Liquid Crystallinity in Polymers Principles and Fundamental Properties*, p. 1–438, VCH, New York (1991).

[62] L. Bosio, B. Fayolle, F. Friedrich, F. Lauprêtre, P. Meurisse, C. Noël, J. Virlet. In *Liquid Crystals and Ordered Fluids*, A.C. Griffin, J.F. Johnson (Eds), Vol. 4, pp. 401, Plenum, New York (1985).

[63] C.K. Ober, J.-I. Jin, R.W. Lenz. *Polym. J.*, **14**, 9 (1982).

[64] G. Vertogen, W.H. de Jeu. *Thermotropic Liquid Crystals Fundamentals*, p. 47, Springer-Verlag, Berlin (1988).

[65] E. Chiellini, G. Galli, A.S. Angeloni, D. Caretti, M. Laus. *Liq. Cryst.*, **5**, 1593 (1989).

[66] A. Blumstein (Ed). *Polymeric Liquid Crystals*, pp. 1–457, Plenum, New York (1985).

[67] G.W. Gray, J.W.G. Goodby. *Smectic Liquid Crystals, Textures and Structures*, pp. 1–162, Leonard Hill, Glasgow (1984).

[68] D. Demus, L. Richter. *Textures of Liquid Crystals*, pp. 1–219, Verlag Chemie, Weinheim (1978).

[69] W.R. Krigbaum. *J. appl. Polym. Sci, appl. Polym. Symp.*, **41**, 105 (1985).

[70] A.A. Collyer. *Mater. Sci. Technol.*, **5**, 309 (1989).

[71] H. Finkelmann. In *Thermotropic Liquid Crystals,* Crit. Rep. Appl. Chem. 22, G.W. Gray (Ed) p. 145, Wiley, New York (1987).